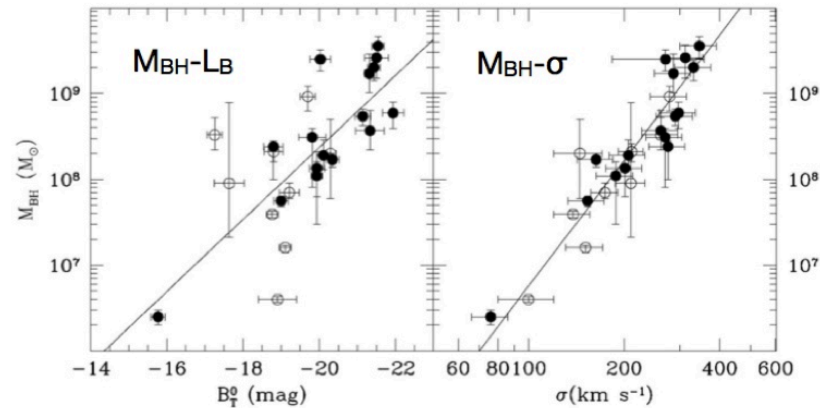# Accreting Black Holes during cosmic time and SAFARI
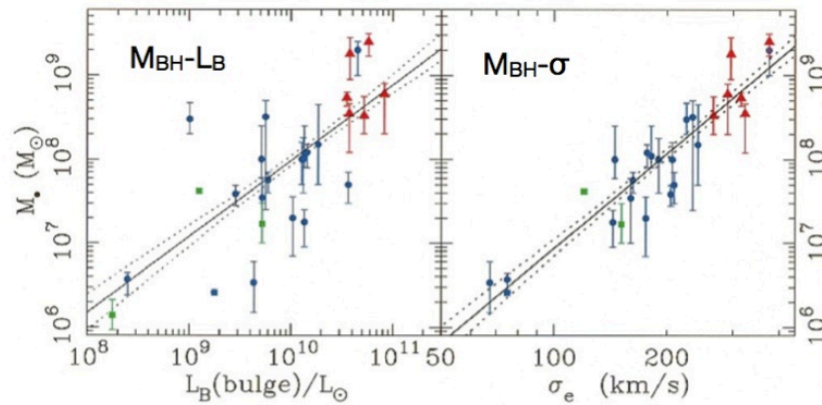
Fabio La Franca

Universita` Roma Tre

Gabriele Melini, Fabrizio Fiore (OAR), …

AGN-Galaxy co-evolution

Figure 5.3: Scaling relation between M_{BH} and M_* for obscured AGN at z ~ 1.3-2.5 with a color-code as explained in the inset of the plot. The solid line is the local relation from Sani et al. (2011), while the dashed one is from Häring & Rix (2004). As comparison, we report with gray asterisks the sample of unobscured AGN at 1.2 < z < 2.1 from Merloni et al. (2010) for which we re-computed the BH masses as explained in Sec. 5.3.

Figure 1.4: Scaling relations between the black hole mass and the properties of the spheroid, as found by Ferrarese & Merritt (2000) and by Gebhardt et al. (2000)
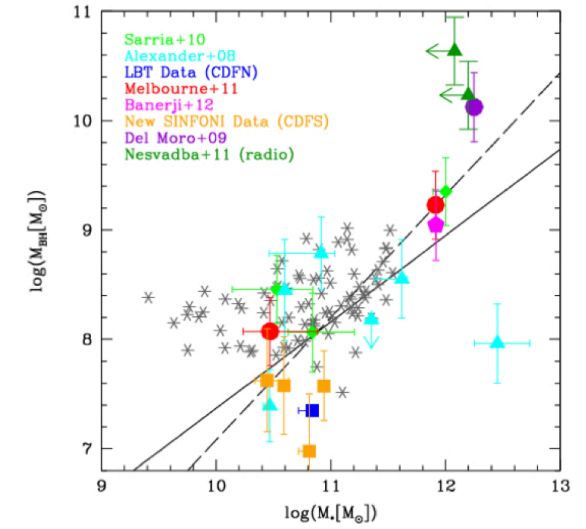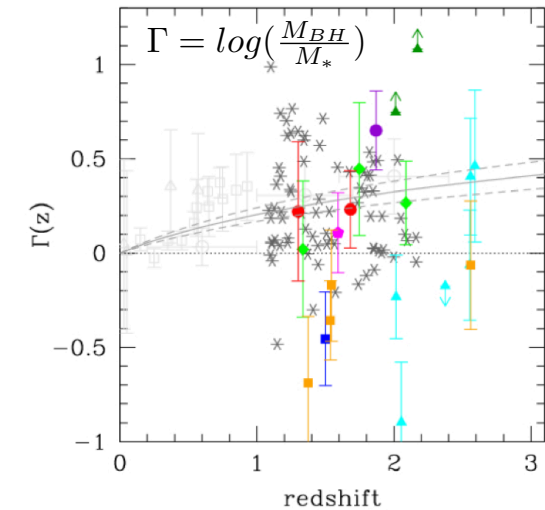

Figure 5.4: Redshift evolution of the offset measured for our AGN sample from the local M_{BH}-M_* relation. Different colors and symbols correspond to the different sub-samples (as in fig 5.3) while light and dark grey symbols show for comparison samples of type-1 AGN from the literature: triangles are from Woo et al. (2008); squares from Salviander et al. (2007), circles from Peng et al. (2006) and asterisks from Merloni et al. (2010). Solid grey line shows the best fit obtained by Merloni et al. (2010): $\Gamma(z) = \Delta \log(M_{BH}/M)(z) = 0.68 \pm 0.12 \log(1+z)$.

AGN-Galaxy co-evolution

$$M_{BH}$$

Accretion Rate
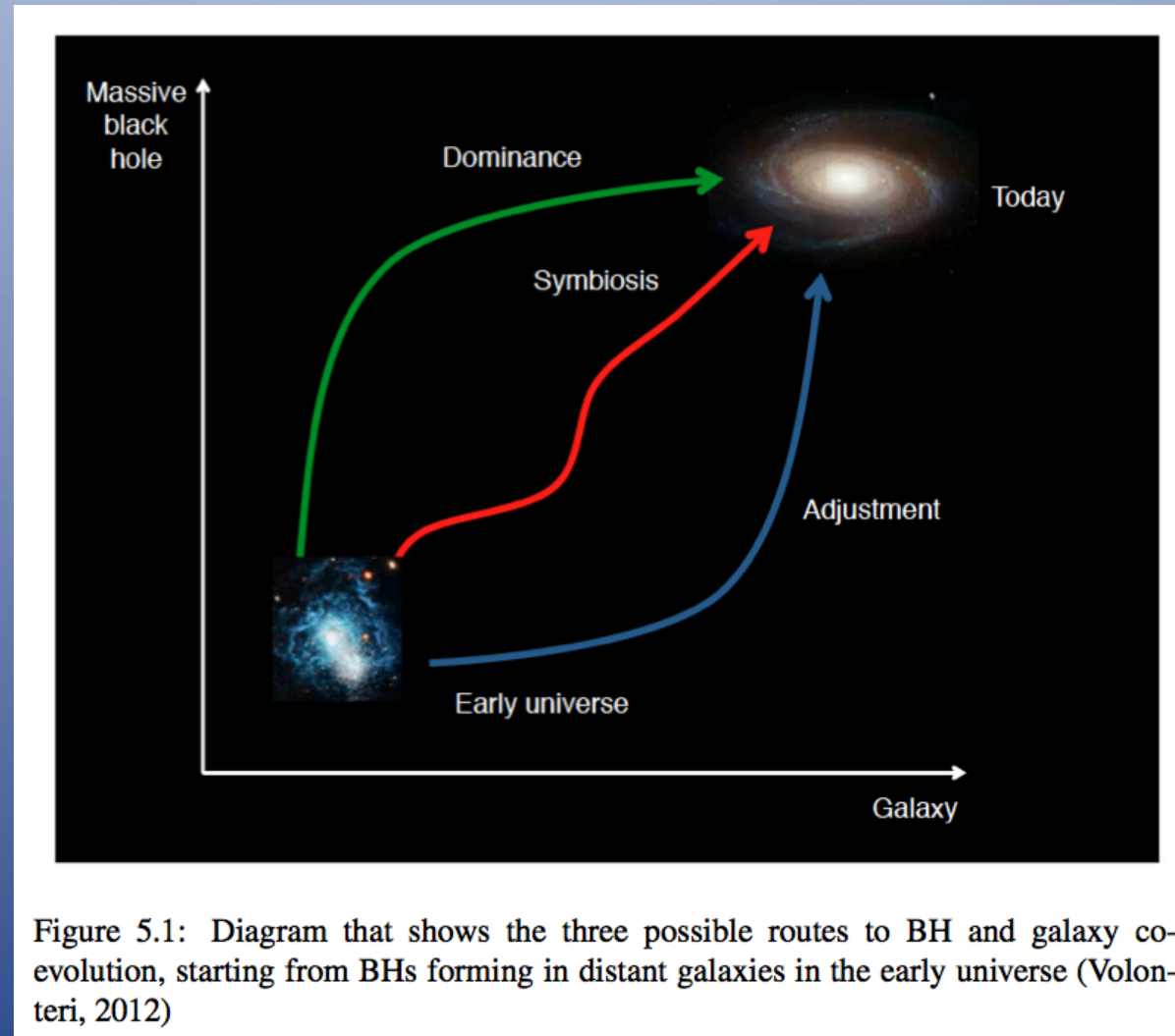
$$\frac{dM_{BH}}{dt}$$

Figure 5.1: Diagram that shows the three possible routes to BH and galaxy co-evolution, starting from BHs forming in distant galaxies in the early universe (Volonteri, 2012)
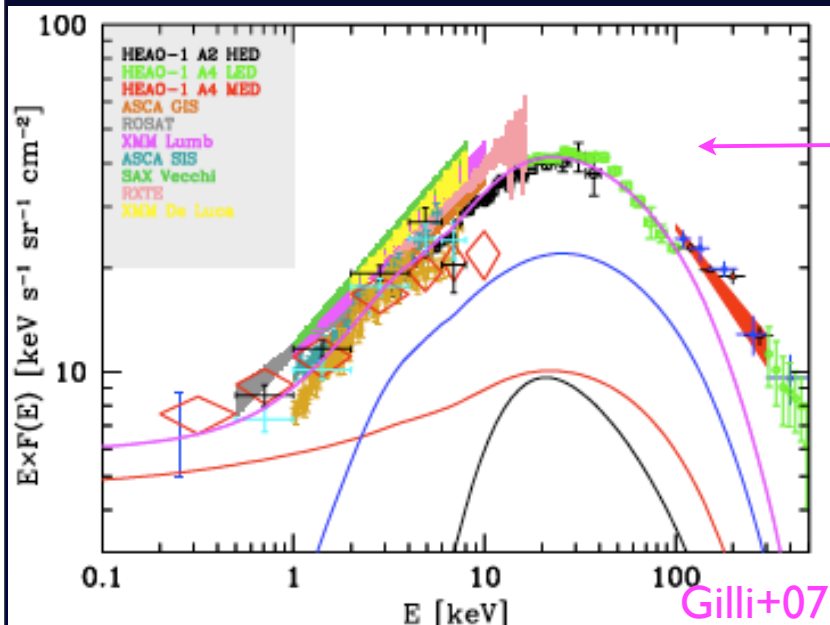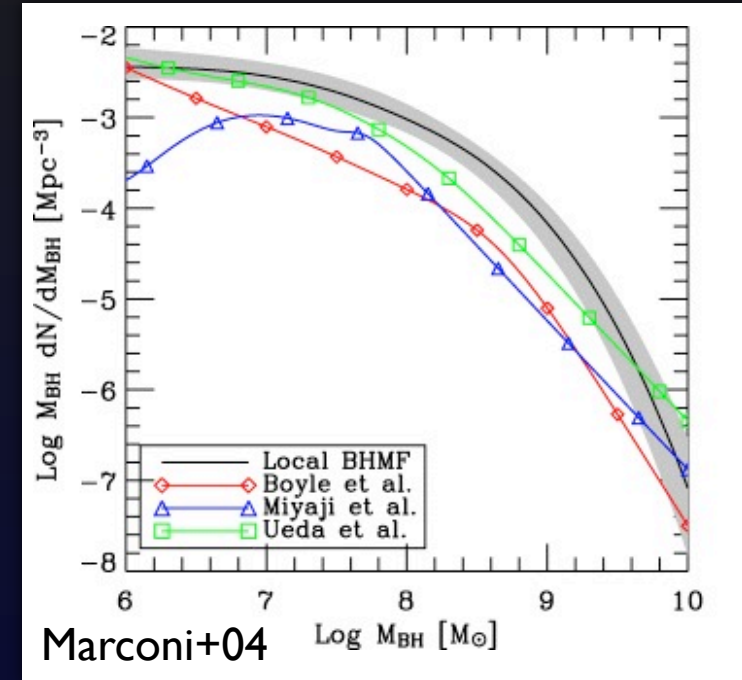
$$M_*$$

SFR: $\frac{dM_*}{dt}$
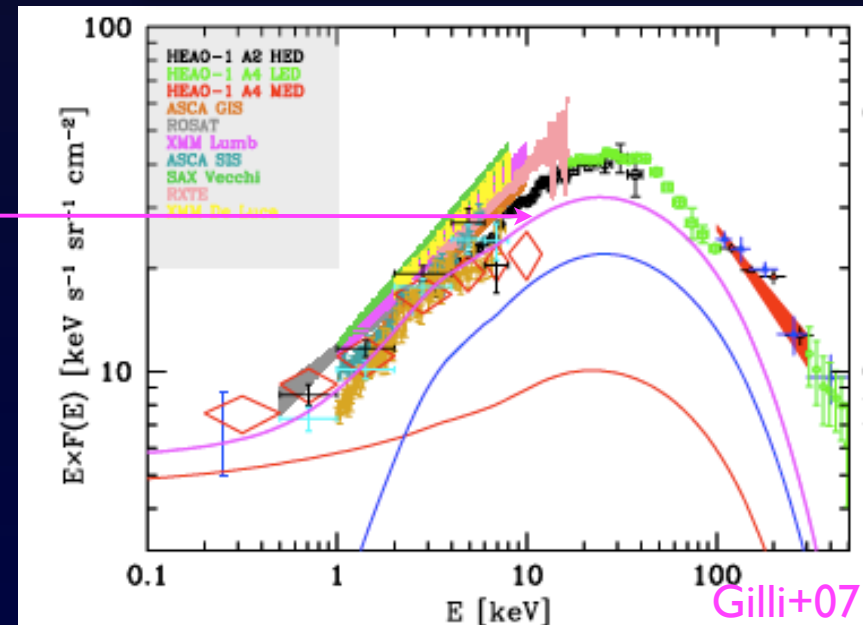
Hints on missing BH?

The BH mass function obtained from the AGN LF is a factor of 2 lower than the local BHMF (which comes from BH-galaxy scaling relations).

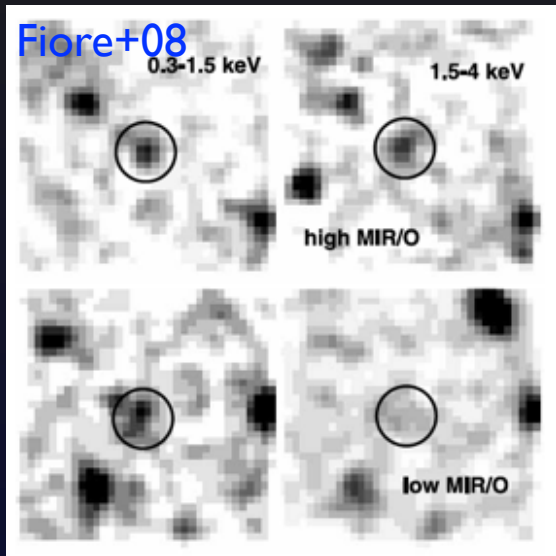X-ray background synthesis models predict a density of CT AGN similar to the density of thin sources.

how can we detect this missing population?

Marconi+04

with CT

without CT

Gilli+07

Gilli+07

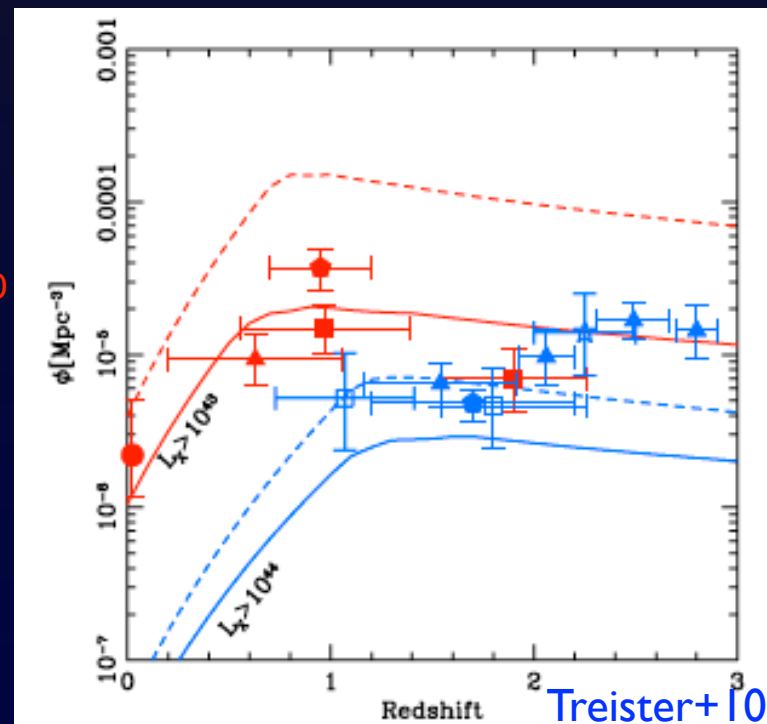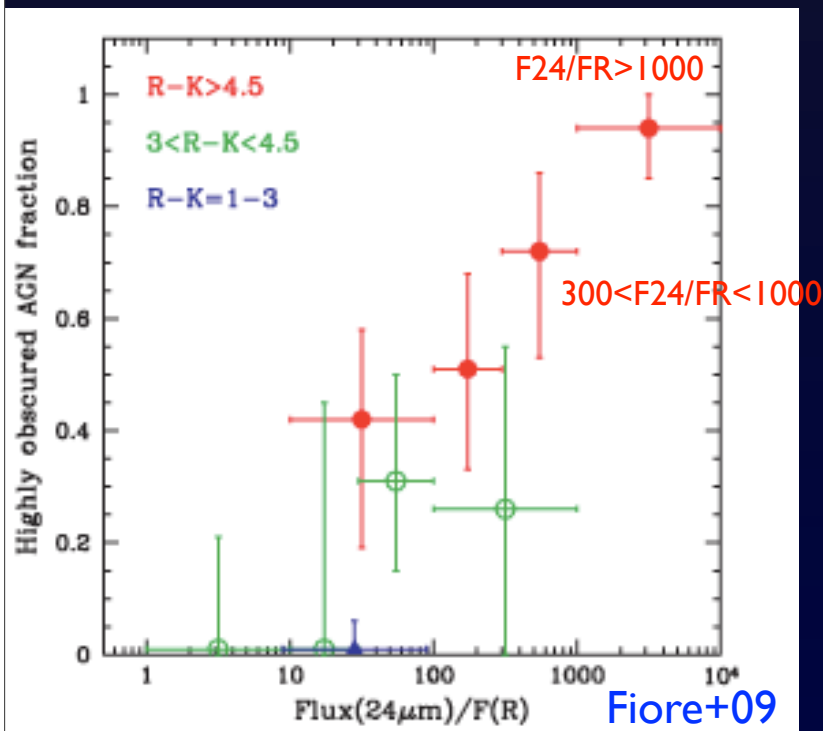# Mid-IR selections

Fiore+08

0.3-1.5 keV   1.5-4 keV
high MIR/O
low MIR/O

Blocked radiation is reprocessed by dust at MIR wavelengths: it is possible to recover obscured AGN by selecting bright IR samples (with faint optical/UV emission)

It has been shown that sources with high F24/FR ratio have hard X-ray emission

Martinez-Sansigre+05, Daddi+07, Dey+08, Fiore+08, Fiore+09, Treister+10, Luo+11

R−K>4.5
3<R−K<4.5
R−K=1−3
F24/FR>1000
300<F24/FR<1000

Highly obscured AGN fraction
Flux(24µm)/F(R)
Fiore+09

$\phi[Mpc^{-3}]$
$L_X>10^{45}$
$L_X>10^{44}$
Redshift
Treister+10

Alexander+11

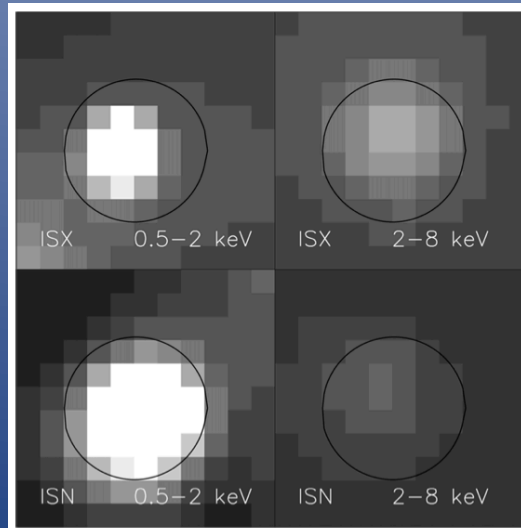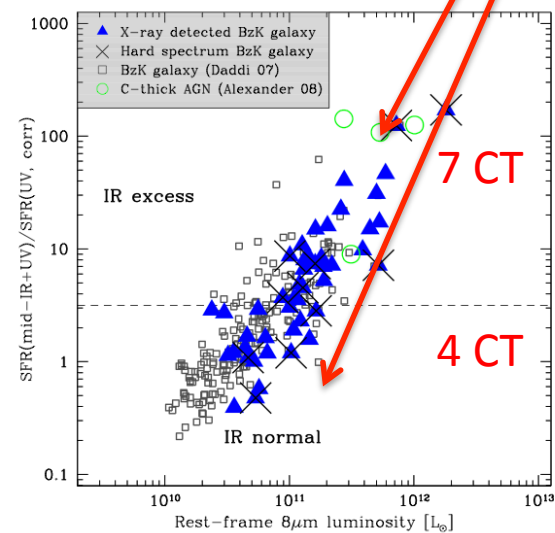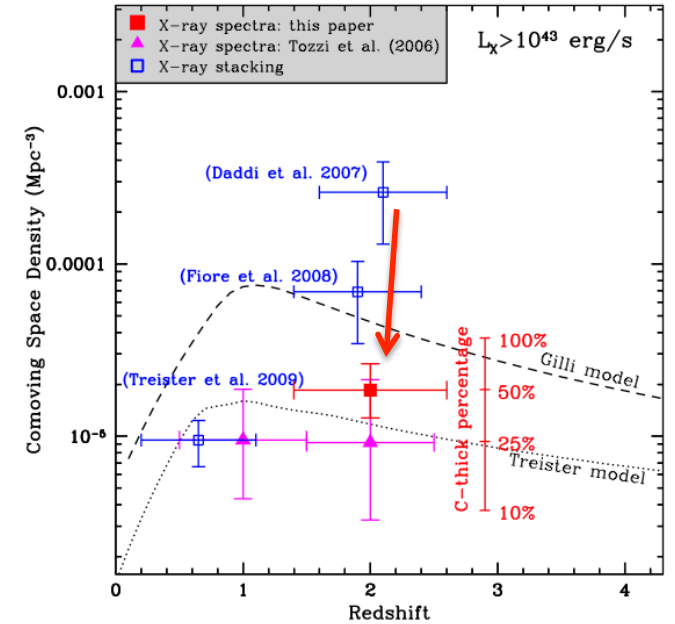CDFS + 4 Ms Chandra

222 BzK galaxies with K<22 and z~2

Revise the work by Daddi+07: less CT AGN found
>10 times lower space densities

Less efficiency in selecting CT AGN
among the IRX BzK galaxies

"Our constraints do not yet support the hypothesis that
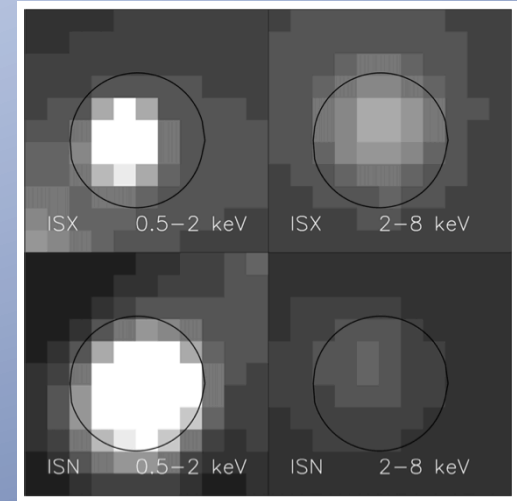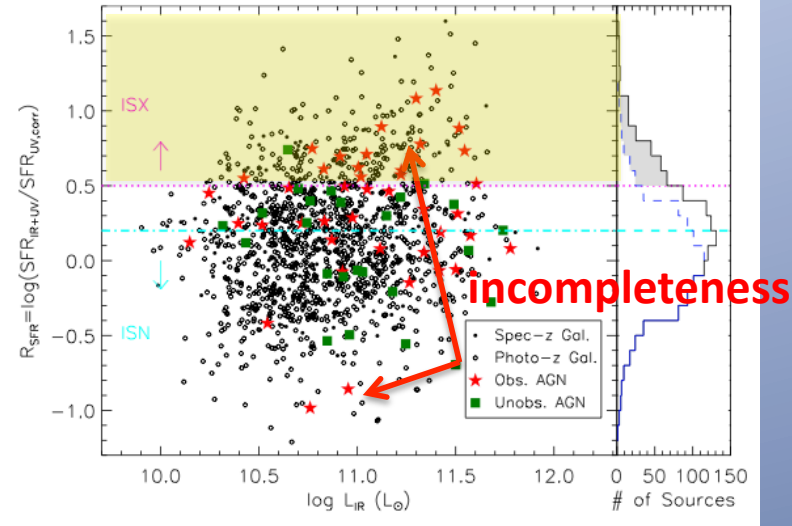Cthick AGN outnumber Cthin AGN at high-z"

7 CT

4 CT
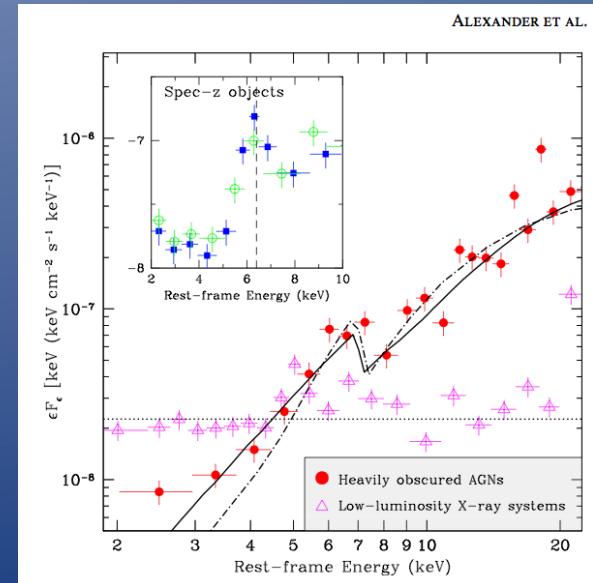
Luo+11

Sample: CDFS+ECDFS

242 ISX sources, 0.5<z<1

ISX: SFRs >3.2 higher than derived from UV corrected for extinction

74% host obscured AGNs
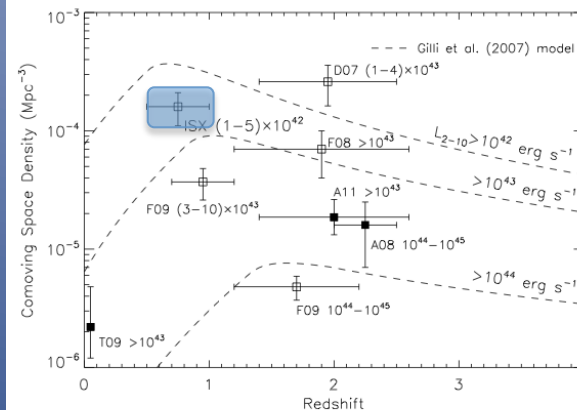
of which 80% are CT

Figure 5. Space density of CT AGNs in the ISX sample. Also shown are the CT AGN space densities in some previous IR-based studies: Daddi et al. (2007, D07), Alexander et al. (2008, A08), Fiore et al. (2008, F08), Fiore et al. (2009, F09), and Alexander et al. (2011, A11). We also include the local CT AGN density from Treister et al. (2009, T09). The redshift error bars indicate the red-shift ranges of the samples, and the intrinsic 2–10 keV luminosity range of each sample is also shown. Note that the Alexander et al. (2008) and Alexander et al. (2011) data points were derived from spectroscopically (X-ray and/or IR) identified CT AGNs, the Treister et al. (2009) data point was derived based on a sample of local CT AGNs, and the other studies are based on X-ray stacking analyses of X-ray undetected candidates. The dashed curves are the predicted space densities of CT AGNs for different X-ray luminosity lower limits from the Gilli et al. (2007) population-synthesis model. Note that the various data points and model predictions have been derived with different underlying assumptions and are thus not strictly comparable.
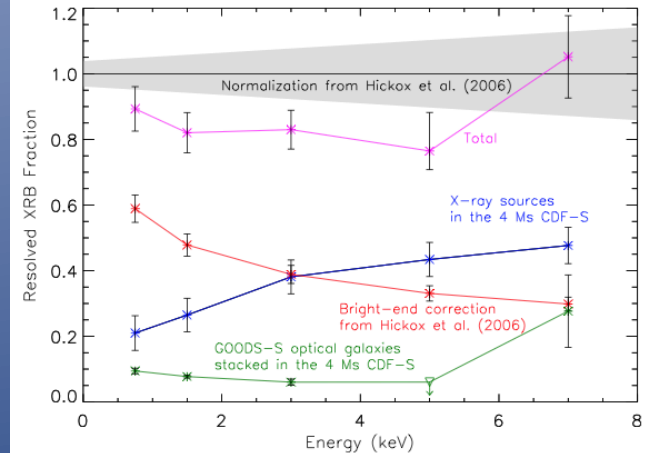
Figure 6. Resolved fractions of the XRB in five energy bands between 0.5 and 8 keV. The total XRB intensities are from Hickox & Markevitch (2006) with uncertainties indicated by the gray region. The stacked contributions from X-ray sources in the 4 Ms CDF-S, bright-end correction, GOODS-S optical galaxies, and the sum of the above are shown by blue, red, dark green, and magenta data points, respectively. Note that the stacked signal for the optical galaxies in the 4–6 keV band did not yield a significant detection and thus a 3σ upper limit on the resolved fraction was calculated (triangle with a downward arrow). The upper limit was used to derive the upper error when calculating the total resolved fraction in this band. For the other data points, 1σ errors are shown. The contribution from the ISX objects is <1.2% in the 6–8 keV band and is not shown.

Olsen+12

CDFS

Mass complete sample: M>5x10^{10} Msol, 1.5<z<2.5
Evidence for a X-ray excess indicative of low-luminosity AGN

As many as 70-100% of quiescent galaxies host an AGN
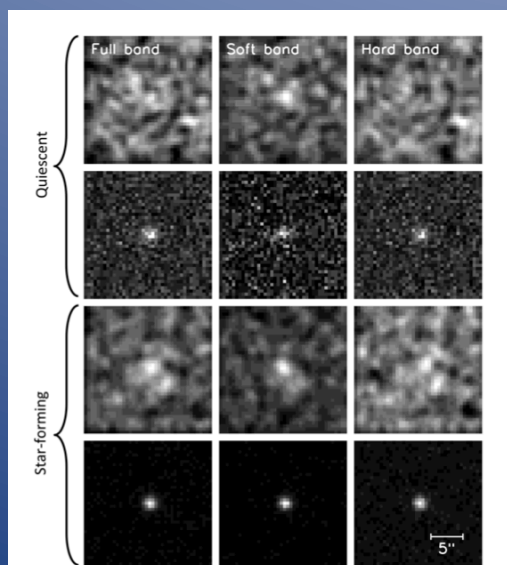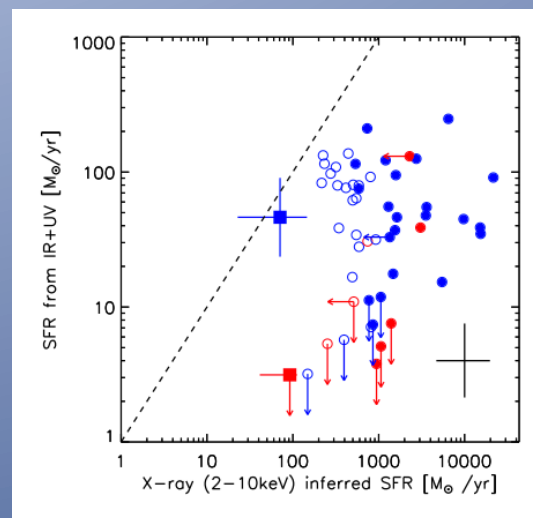**43-65% of star forming galaxies host an AGN**

Figure 1. Stacked, background-subtracted and exposure-corrected 20″ × 20″ images in the three energy bands (columns) for the individually non-detected (top row) and detected (bottom row) quiescent and star-forming galaxies. Images of the non-detections have been smoothed with a Gaussian of width 2 pixels.

|	Quiescent (27)	Star-forming (96)
Luminous AGN	5	22
Low-luminosity AGN	2 (det)	19 (det)
	12 − 19 (non-det)	0 − 21 (non-det)
Luminous AGN fraction	19 ± 9%	23 ± 5%
Total AGN fraction	70 − 100%	43 − 65%

Table 3

X-ray derived AGN numbers and fractions for quiescent and star-forming galaxies, divided into luminous AGN and detected and non-detected low-luminosity AGN.

REVIEW SUMMARY:

X-ray stacking analyses of SED and/or color
selected galaxy samples find evidences of a
large fraction of obscured AGN (accretion)
but the samples are affected by not quantified
incompleteness.

Moreover
it is difficult to separate the star formation from the
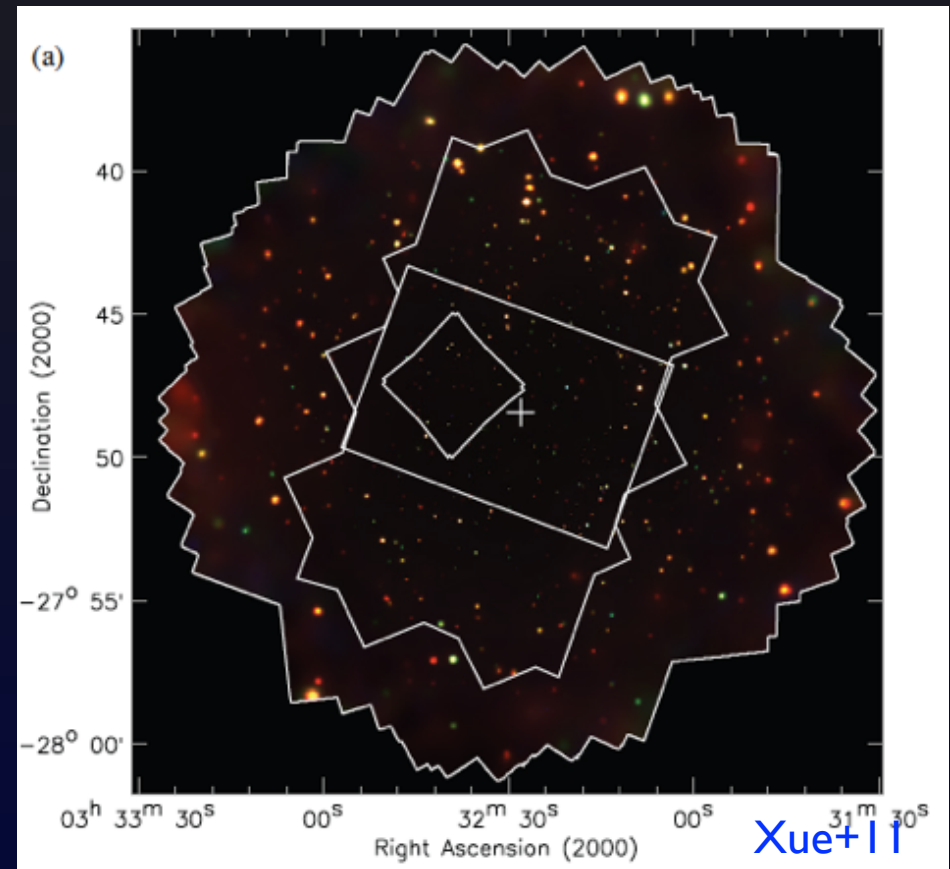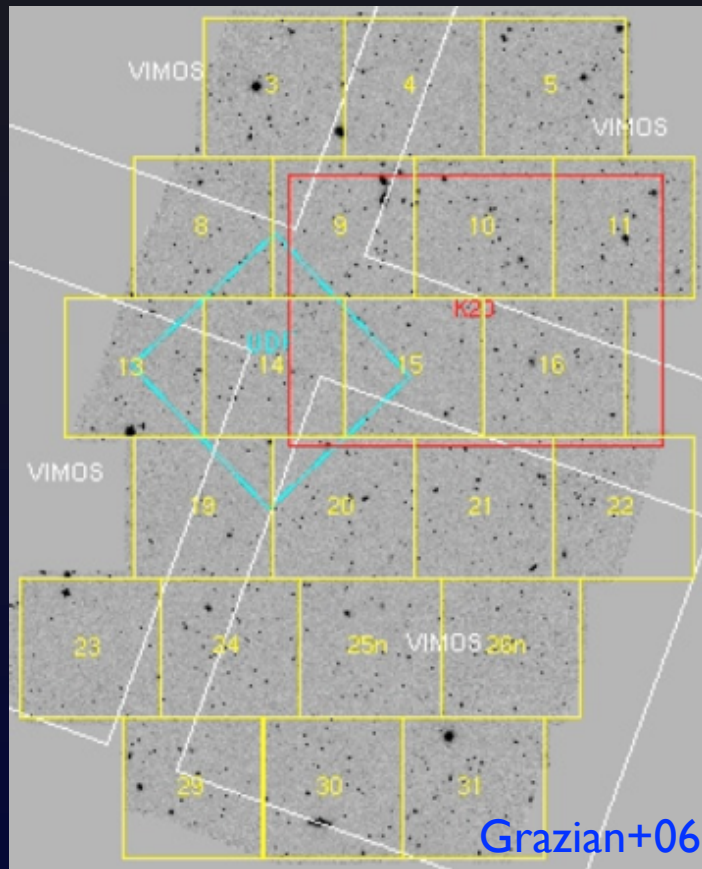accretion in the contribution to the
luminosity budget

Data set: COSMOS
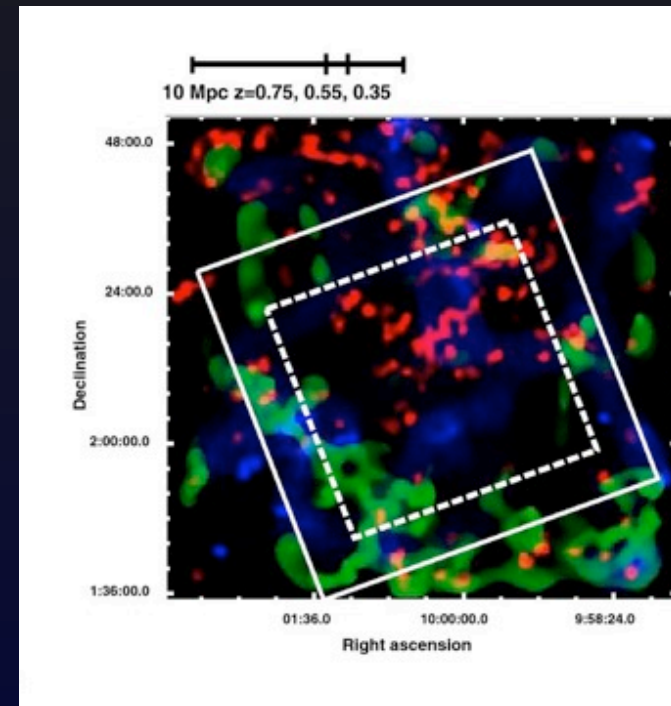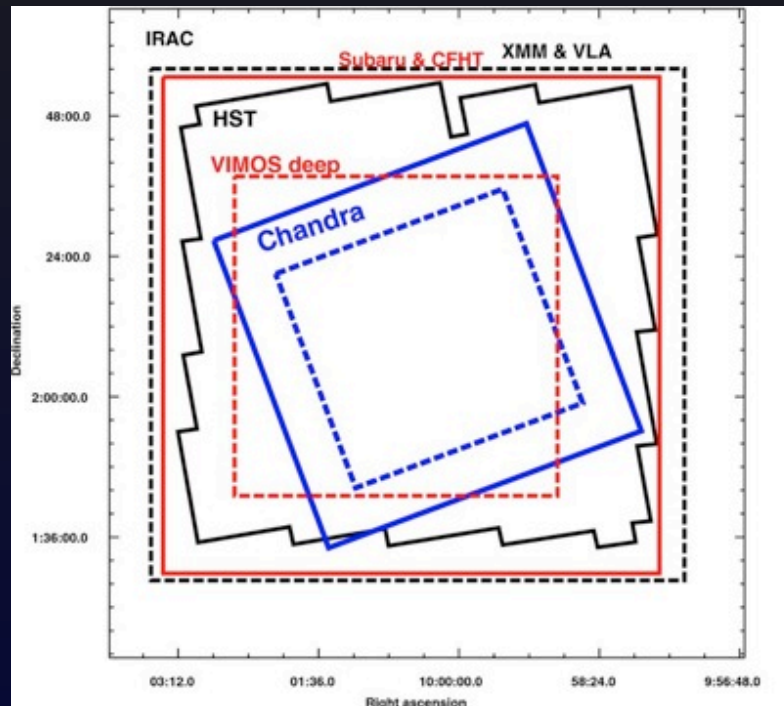
Elvis+09

- ~15000 galaxies with F24>80 uJy (MIPS GO3 survey)
- zspec or zphot available for ~100% of the sample
- multiwavelength data available (X, UV, optical, IR)
- uniform Chandra X-ray coverage over 0.9 deg^2 (~200 ks)

Data set: GOODS-MUSIC

Grazian+06

Xue+11

- 0.143 deg^2 area (near-IR observations by VLT/ISAAC)
- ~1800 galaxies over F24=20 uJy
- zspec/zphot available
- deep CDFS X-ray data available (4 Ms; Xue+11)

Data set: SED fitting
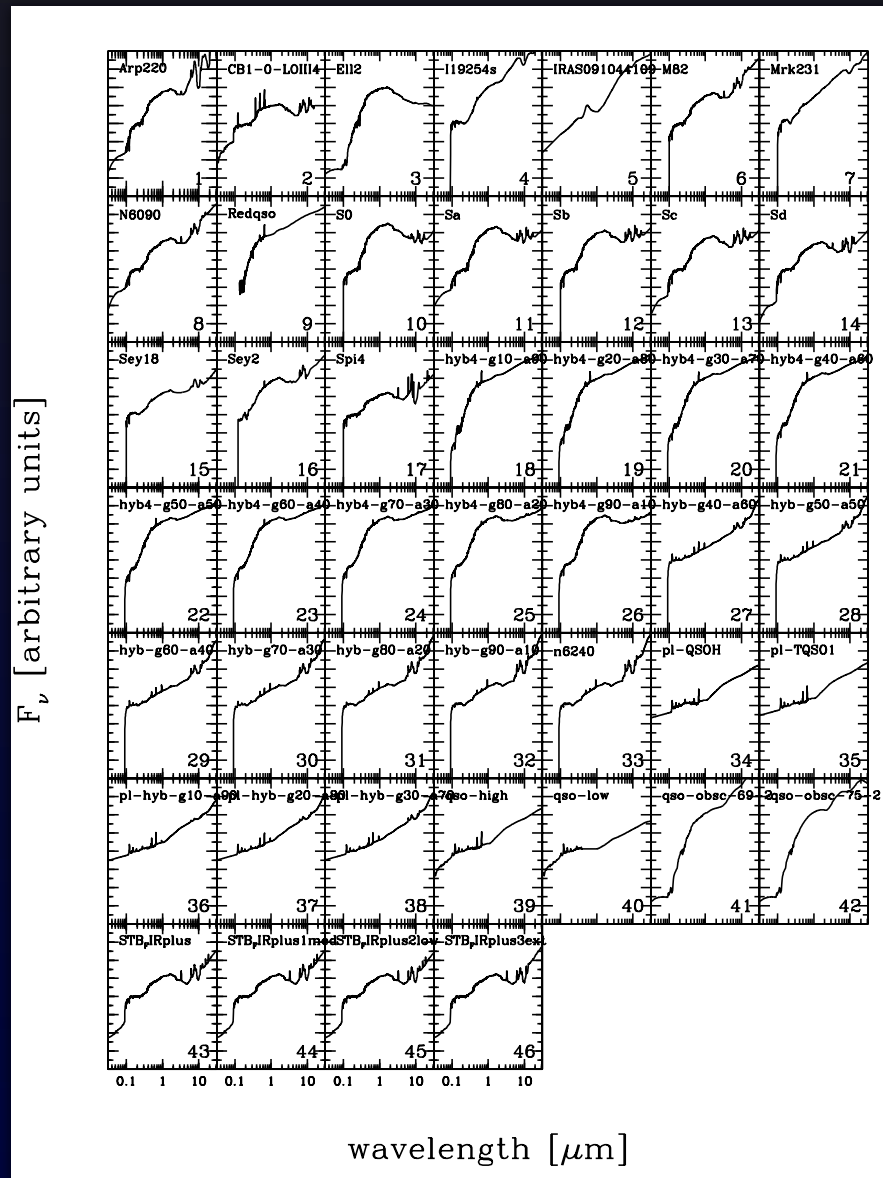
Library of 46 template SED from Polletta+07, Salvato+09, Fiore+09 and Sacchi08.

We fitted the IRAC (3.6, 4.5, 5.8 and 8.0 um) and MIPS 24 um data points with LePHARE code (Arnouts+99, Ilbert+06) to derive 5.8 um luminosity for each source.

Redshifts fixed to spec or phot values depending on quality (and availability) of spec estimations.